A RESEARCH ON WASTE-GATED TURBINE PERFORMANCE UNDER UNSTEADY FLOW CONDITION

Q Deng
Powertrain Vehicle Research Centre
Department of Mechanical Engineering
University of Bath, BA2 7AY, Bath,UK
Email:qd226@bath.ac.uk

R. D. Burke
Powertrain Vehicle Research Centre
Department of Mechanical Engineering
University of Bath, BA2 7AY, Bath,UK
Email: R.D.Burke@bath.ac.uk

Q Zhang
Powertrain Vehicle Research Centre
Department of Mechanical Engineering
University of Bath, BA2 7AY, Bath,UK
Email: Q.Zhang@bath.ac.uk

Ludek Pohorelsky
Honeywell Technology Solutions, CZE
Turanka 100, 62700 Brno, Czech Republic
Email: Ludek.Pohorelsky@Honeywell.com

ABSTRACT

Turbochargers are key components of engine air-paths that must be carefully considered during the development process. The combination of fluid, mechanical and thermal phenomenon make the turbocharger a highly dynamic and non-linear modelling challenge. The aim of this study is to quantify the dynamic response of the turbocharger system across a frequency spectrum from 0.003Hz to 500Hz, i.e. for exhaust gas pulsation in steady state, load steps and cold start drive cycles, to validate the assumption of quasi-steady assumptions for particular modelling problems.

A waste-gated turbine was modelled using the dual orifice approach, a lumped capacitance heat transfer model and novel, physics-based pneumatic actuator mechanism model. Each sub-model has been validated individually against experimental measurements. The turbine inlet pressure and temperature and the waste-gate actuator pressure were perturbed across the full frequency range both individually and simultaneously in separate numerical investigations. The dynamic responses of turbine housing temperature, turbocharger rotor speed, waste-gate opening, mass flow and gas temperatures/pressures were all investigated.

The mass flow parameter exhibits significant dynamic behaviour above 100Hz, illustrating that the quasi-steady assumption is invalid in this frequency range. The waste-gate actuator system showed quasi-steady behaviour below 10Hz, while the mechanical inertia of the turbine attenuated fluctuations in shaft speed for frequencies between 0.1-10Hz. The thermal inertia of the turbocharger housing meant that housing temperature variations were supressed at frequencies above 0.01Hz.

The results have been used to illustrate the importance of model parameters for three transient simulation scenarios (cold start, load step and pulsating exhaust flow).

1. INTRODUCTION

As turbochargers have a critical role in engine downsizing, the good understanding of turbocharger performance on-engine is vital at many stages of the engine and vehicle design process. The engine subjects the turbocharger to a range of highly transient

boundary conditions such as the turbulent and pulsating flows from the engine exhaust at high frequencies and the changes in engine coolant and oil temperatures at low frequencies [1]. These operating conditions excite the inherent dynamics of the turbocharger due to its internal volumes, mechanical and thermal inertias. Therefore, a turbocharger-engine system represents a multi-frequency, non-linear modelling problem. Creating a single turbocharger model capable of capturing all these effects together remains challenging. However, under different operating conditions, certain dynamic effects will be more or less important. The aim of this work is to quantify the turbocharger dynamic behaviour across a wide frequency spectrum to advise the key model features that should be prioritised for particular modelling tasks.

2. BACKGROUND

Research on turbine transient performance has typically focussed on a particular operating condition, corresponding to a particular frequency range, such as pulsating flows from the engine valve events or changes in engine speed and torque. These fields first be considered individually.

2.1 Unsteady flow effects on Turbine performance

The engine will create a pulsating flow of exhaust gases at frequencies in the region of 25-300Hz depending on the number of cylinders and the operating speed. Previous research in this domain has sought to better design and model turbines for operation in these conditions, with a particular focus on 1D gas dynamic models for engines [2, 3]. These models suffer in accuracy due to the quasi-steady assumption inherent to the characteristic maps used as a basis for turbine models [4, 5]. Aymanns et al. [6] used computational fluid dynamic (CFD) simulations to investigate the turbine performance both in quasi-steady and transient ways. They indicated that there were three possible reasons why the quasi-steady assumption was erroneous for turbine simulations:

1. The characteristic maps are insufficient to describe the mass accumulation phenomena in volute and impeller;
2. The energy conversion due to the changes in aero-dynamics and variations of flow cross section cannot be represented
3. The interactions between exhaust manifold gas dynamics and turbine are not well captured.

According to the comparison between steady-state and transient simulation, 40% difference was captured for the flow capacity. This suggests that the use of the quasi-steady assumption would significantly underestimate turbine flow, a trend supported by other authors [7-12]. There is general agreement that the transient behaviour results from the internal volumes of the turbine. The largest contribution comes from the volute: a hysteresis loop of the mass flow parameter against pressure ratio is evidence of the filling and emptying of the internal volumes [4, 13-16].

The importance of these flow pulsations has been analysed using the Strouhal number to describe the frequency variations in a non-dimensional format [7, 8, 17]. The Strouhal number is a non-dimensional quantity expressing the ratio of wave travel time in a

particular geometry to the period of the wave. However, Copeland et al. [1] suggested that both frequency and amplitude would be important and proposed an amplitude factor that would be combined with the Strouhal number for a mode complete evaluation of the transient response.

To improve upon the characteristic maps in engine system simulations, Aymanns et al. [6] suggested that the maps be combined with a reasonable volute model to overcome the deviations caused by the mass flow storage phenomenon. To preserve the acoustic behaviour, nozzles or orifices were used to represent the turbine expansion process [18]. To avoid choke in the model, either one nozzle is used representing half the total expansion [19, 20] or two orifice in series to achieve the high pressure ratios typically seen across radial turbines [3, 21]. An intermediate volume allows the model to represent the mass flow storage phenomenon within the wheel itself. The cross sectional area of each nozzle is varied according to the operating points, a process that has more recently been extended to model variable geometry turbines (VGT) [22-24].

2.2 Mechanical effects

The key mechanical elements affecting turbine performance are the inertia of the turbine rotor and the waste-gate actuator. Capobianco and Marelli [16] investigated the turbine behaviour when subjected to the pulsating flows under three different frequencies (40/70/100Hz). Fluctuations in rotational speed were observed and related to the mass flow pulse frequencies. The amplitude of speed fluctuation was related to the pulse frequency - higher frequency resulted in lower level in amplitude [25]. Several studies [26-29] have been published for pneumatic waste-gate actuator dynamic modelling. The studies highlighted the need for accurate estimation of friction in the mechanism and aerodynamics of the valve. These studies have shown specific responses of waste-gate opening to step and ramps inputs, to the authors' knowledge, a broad analysis across the frequency range has not been presented.

2.3 Heat transfer effects

Several authors [30-32] have studied heat flows in turbochargers. The heat transfer occurs through the turbine housing, between the different working fluids (intake air, exhaust gases, lubricant, coolant and ambient cooling air) [30], Heat transfer is problematic during engine development because temperatures are used to measure work transfers in the compressor and turbine, and if heat transfers are ignored, these temperatures will cause inaccuracies in efficiency measurements. At high turbocharger speeds the situation is less critical as heat transfer represents only a small fraction of total enthalpy changes [30, 33-37], at low speeds this is not the case [38]. Heat transfer in the turbocharger also directly affect the exhaust temperature provided to the after-treatment devices; this is critical during the warm up which represent a very low frequency transient.

Characteristic maps typically ignore heat transfer effects and consequently are only valid in regions where heat transfer is small compared with work transfer. In low speed regions, turbine efficiency can be overestimated by more than 20%points [34]. At these operating points, heat transfer can represent 70% of the total enthalpy change in the turbine [30]. Most researchers agree that the

influence of heat transfer on the aerodynamic performance is negligible, and the issues are mainly a consequence of the experimental methods used to measure isentropic efficiency for modelling purposes. Lumped capacitance model have been proposed that calculate the convective, conductive and radiation heat transfers in a simple yet effective way for both steady and transient conditions [39, 40].

This paper combines these three elements together in a single model to investigate the transient behaviour of a waste-gated turbine. After building the model and validating the individual components, firstly temperature and pressure boundary conditions were excited individually using sine-wave functions with frequencies ranging from 0.003Hz to 500Hz. This captured fundamental physical behaviour. Secondly, simulations were undertaken with simultaneous excitation of boundary conditions to better approach realistic engine operating conditions. Finally, frequency analysis was undertaken better appreciate the implications for turbocharger turbine modelling. .

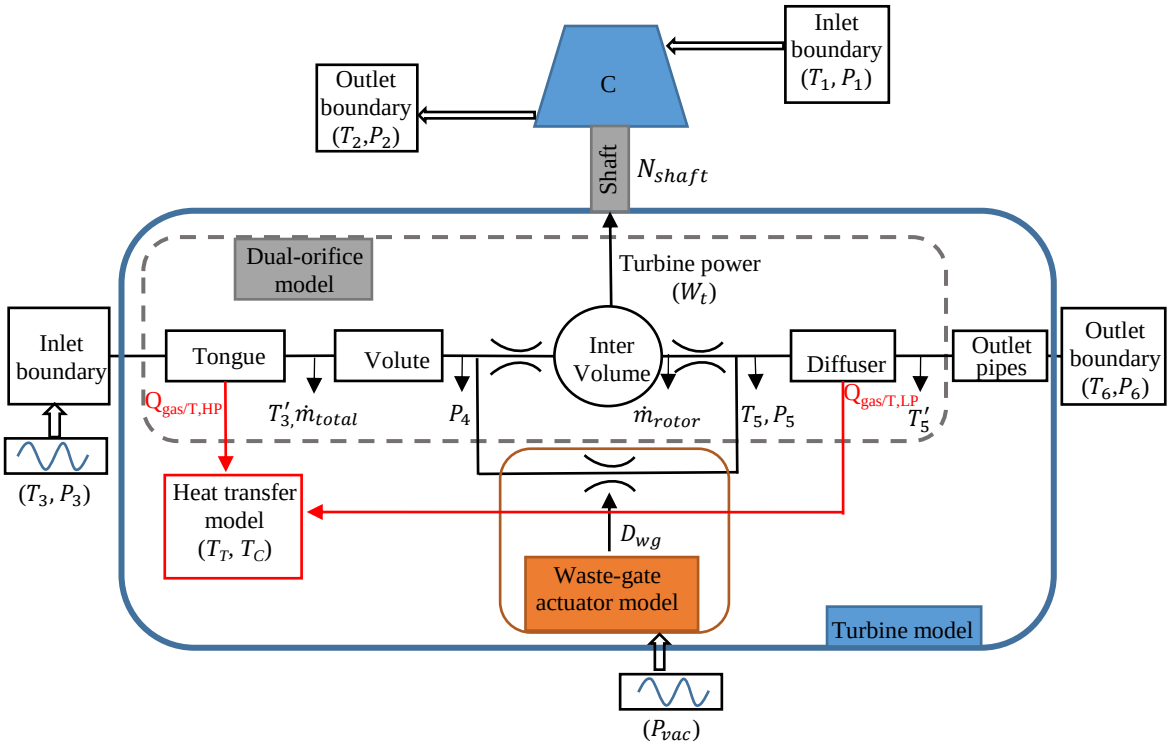

Figure 1: Schematic overview of turbine model showing flow paths, heat transfer and waste gate model structure. Perturbed boundary conditions are turbine inlet temperature and pressure (T_3, P_3) and waste gate actuator vacuum pressure (P_{vac})

The results from this study will:

1. Characterise the turbocharger transient response;
2. Identify the most critical dynamic phenomena at particular excitation frequencies.

The results can be used by practicing engineers to determine the most important dynamic model parameters for a particular simulation task.

3. METHODOLOGY

In this section the model structure and validation is described before detailing the simulation conditions used to assess the frequency response of the turbocharger turbine. The model was compiled in Gamma Technologies GT Power to make use of the mathematical solver and basic models for compressible flows in pipes and orifices.

3.1 Model structure

A full turbocharger model was created by combining a dual-orifice turbine model [24], lumped capacitance heat transfer model [39] and new waste gate mechanical model. Figure 1 shows the schematic of the model and each sub-model is detailed in the subsequent sections. The boundary conditions that have been varied for the turbine inlet pressure and temperature (P_3, T_3) and the waste-gate actuator supply vacuum pressure (P_{vac}). The turbine outlet pressure was also imposed as a constant at 1 bar. As the focus of the research is on the turbine behaviour, a simple, quasi-steady compressor model was used to load the turbine using a characteristic map approach. The boundary conditions for compressor inlet temperature and pressure, T_1 and P_1, were set to be a constant 298K and 1bar respectively whilst the compressor outlet pressure, P_2, was set to 1.9 bar. Both outlet temperature, T_2 and T_6, were calculated parameters. The model outputs were the turbine housing temperature (T_T), gas temperature/pressure ($T_{3'\text{-}6}$ and $P_{3'\text{-}6}$), shaft speed (N_{shaft}), area of waste-gate (A_{wg}) and mass flows ($\dot{m}_{total}$ and $\dot{m}_{rotor}$).

The mechanical power created by the turbine was calculated on an instantaneous basis using equations 1 and 2, where instantaneous rotor mass flow ($\dot{m}_{rotor}$) and specific heat capacity (c_p) was taken in the inter volume location shown in figure 1.

$$W_t = \dot{m} c_p (T_5 - T_3') \quad (1)$$

$$T_5 = T_3' \left(1 - \eta_t \left(1 - \left(\frac{P_4}{P_5} \right)^{\frac{\gamma}{\gamma - 1}} \right) \right) \quad (2)$$

Mechanical power was extracted from the gas flow in the intermediate volume by virtue of an enthalpy reduction of the gas. Compressor power was used to load the turbine and the shaft speed was solved numerically based on a shaft power balance shown in equation 3. The friction loss was counted in the turbine efficiency map.

$$\dot{N}_{shaft} = \frac{W_t - W_c}{N_{shaft} \cdot I_{shaft}} \quad (3)$$

3.1.1 Turbine dual-orifice model

The turbine flow path was represented by the dual-orifice model proposed by Serrano et al. [24]. The internal volume of the turbine was divided to four parts: tongue (A), volute (B), rotor (C) and diffuser (D) as shown in figure 2.

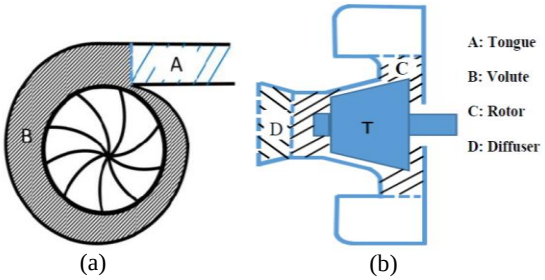

Figure 2: Schematic diagram of volumetric breakdown for dual-orifice turbine model

The turbine tongue (A), volute (B) and diffuser (D) were described by one dimensional pipes with the same volume as their respective 3D shapes. Turbine tongue and diffuser were modelled by tapered pipes based on the real geometry of the turbine. The turbine volute was simplified to be a straight pipe, having the same diameter of the outlet of the tongue and length to satisfy the volume criterion. The intermediate volume was sized to be the same total volume as volume C. The effective area of stator and rotor orifices, which are a function of reduced speed and pressure ratio, were derived from the turbocharger characteristic maps. The extrapolation of turbine map and the effective area maps of stator and rotor were obtained based on the methods proposed in [24] and [41].

3.1.2 Heat transfer model

A lumped capacitance heat transfer model proposed by Burke [39], which was a simplified version of the model proposed by Olmeda et al. [42], was used to model the thermal behaviour. The turbine and compressor housings were represented as two thermal nodes which were linked via a conductive resistance representing the bearing housing. Further thermal resistances were used to represent convection and radiation with the surroundings. Figure 3 shows all the heat fluxes considered in the heat transfer model. Convection between the working fluids and the housing nodes was allowed to occur both before and after the expansion and compression processes. The expansion and compression processes themselves were assumed to be adiabatic.

The internal convection was estimated using Newton's law of cooling (equations 4 and 5) where areas A-D correspond to the wetted areas of volumes A-D, as depicted in figure 2. This approach assumes that the wetted areas A-C are exposed to high pressure gas while wetted area D is exposed to low pressure gas.

$$Q_{gas/T,HP} = h_{HP}(A_A + A_B + A_C)(T_3 - T_T) \qquad (4)$$

$$Q_{gas/T,LP} = h_{LP}A_D(T_5 - T_T) \qquad (5)$$

The internal convective heat transfer coefficient was estimated using equation 6, which has been shown to be representative over a range of turbocharger types and sizes [43,44].

$$Nu = 0.38Re^{0662}Pr^{1/3}\left(\frac{\mu_{T_{gas}}}{\mu_{T_T}}\right)^{0.14} \qquad (6)$$

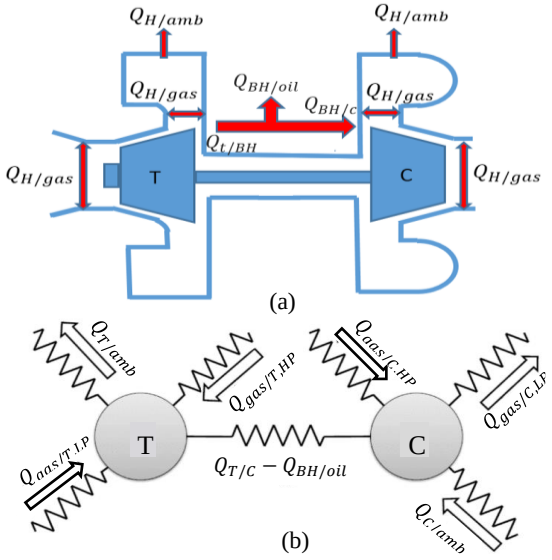

Figure 3: Overview of heat transfer model: (a) schematic of heat transfer process (b) diagram of simplified heat transfer lumped model

The external convective heat transfer coefficient was estimated using equation 7 which was derived by Ericsson [45] and was based on typical convective properties under bonnet and exhaust pipe conditions in vehicle. Radiation heat losses were estimated using equation 8 for a grey body in a large enclosure.

$$h_{T/amb} = 1.25(T_T - T_{amb})^{1/3} \quad (7)$$

$$Q_{rad} = A_{T,external}\varepsilon_T\sigma({T_T}^4 - {T_{amb}}^4) \quad (8)$$

The heat transfer from turbine to bearing housing and oil and from bearing housing to compressor housing were calculated using equations 9-11. The heat flow through from turbine to compressor housing is described as 1D heat conduction using the geometrical and thermal properties of the bearing housing. Heat transfer to oil is assumed to represent a fixed percentage of overall heat transfer from the turbine to compressor as illustrated in figure 3a. This is a further simplification to the model proposed by Olmeda et al. [42] which is suitable for simulations where the turbine housing is predominantly hotter than the compressor housing as is the case in this study.

$$Q_{T/BH} = \frac{A_{BH}k}{l_{BH}}(T_T - T_C) \quad (9)$$

$$Q_{BH/oil} = 0.7 \times Q_{T/BH} \quad (10)$$

$$Q_{BH/C} = Q_{T/BH} - Q_{BH/oil} \quad (11)$$

3.1.3 Waste-gate model

The waste-gate used in this paper was a monoblock spheroid design [46]. The waste-gate model consisted of:

1. The actuator model

2. The waste-gate valve effective area model.

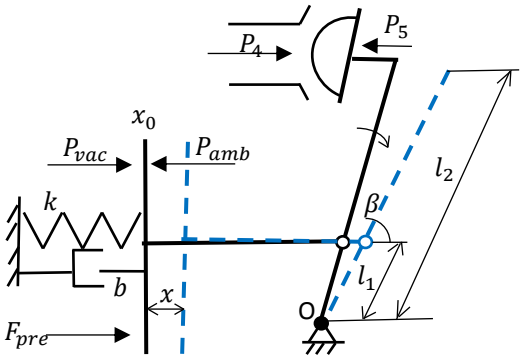

Figure 4. Diagram of waste-gate actuator model (P_4, P_5correspond to the pressures indicated in figure 1)

The waste-gate actuator used by this turbine was a pneumatic actuator driven by vacuum and is shown schematically with the linkage mechanism in figure 4. The waste-gate pivots about point O, and the motion of piston and waste-gate poppet is described by the lengths l_1 and l_2.

Inside the actuator, a spring of stiffness *k* pushes the actuator to its extended position, holding the waste-gate valve open. The spring is pre-loaded and in addition to static friction applies a force F_{pre} to the actuator rod.

When a sufficiently low vacuum pressure P_{vac} is applied to the piston to overcome the spring force, the actuator will move and close the waste-gate. When the piston moves, there is an internal damping effect represented by the parameter *b*. Finally, the pressure ratio over the waste-gate, represented by P_4 and P_5, applies an additional force onto the mechanism.

Applying Newton's second law to the rotation of the waste-gate pivot yields equation 12.

$$I_{wg}\ddot{\beta} = \left[\left(F_{pre} + kx + b\dot{x} + (P_{amb} - P_{vac})A_{piston}\right)l_1 - (P_4 - P_5)A_{valve}l_2\right] sin\,\beta \qquad (12)$$

where l_1 and l_2 refer to those depicted in figure 4.

The inertia of the system was estimated based on the material property and the geometry information. The damping ratio was obtained based on the fitting experimental results.

In the flow model, the waste-gate was modelled as a variable area orifice connected by two pipes. The effective area was calculated by simplifying the 3-D problem to be 2-D calculation: this was illustrated in figure 5.

- D_{wg} and l_1 are the geometry data of waste-gate valve representing the length of waste-gate rod and diameter of waste-gate valve.
- β is the angle of the waste-gate valve which is calculated by the waste-gate actuator model.

In 3-D, the gases should flow between the housing and the spherical waste-gate through a ring like section of varying opening. To estimate the effective area, this was considered as two half rings which correspond to the hashed areas in figure 5b. D_1 and D_2

were calculated according to the coordinates of points 1-5, referred to the location 0 on the

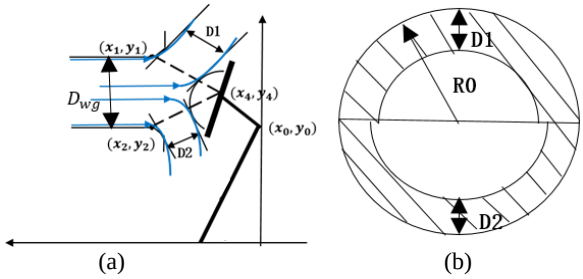

Figure 5: Illustration of waste gate effective area calculation

Waste-gate lever arm, as shown in figure 5. The waste gate are was then calculated using equation 13.

$$A_{wg} = \frac{\pi}{4} D_{wg}^2 = \frac{1}{2}\pi[({R_0}^2 - (R_0 - D_1)^2) + ({R_0}^2 - (R_0 - D_2)^2)] \quad (13)$$

3.2 Model validation

3.2.1 Dual-orifice model

In order to validate the dual-orifice model, 44 operating points were simulated with closed waste-gate covering a broad area of the turbine map. The boundary conditions for the steady state test were set with inlet pressure from 1.3 bar to 3.5 bar and inlet temperature from 600K to 1000K, the distribution of test points on the turbine map is shown in figure 6. The orifice model results were compared to the characteristic map which extrapolated measured data using a modified version of the Jensen & Kristiansen method [47].

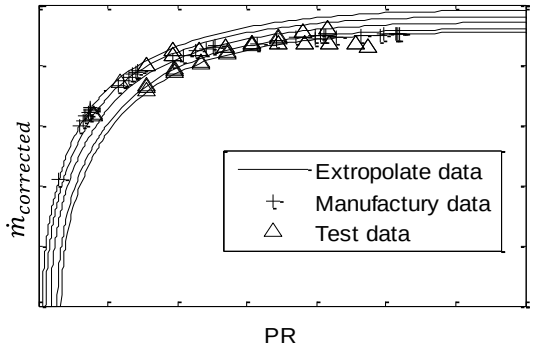

Figure 6: Steady-state test data for turbine performance comparing reference manufacturer map (from Gas stand tests) and simulated test data using the dual orifice model

Figure 7 illustrates the correlation between the two-orifice model and the characteristic map. The maximum errors and coefficient of determination (R^2, equation 14) for each parameter are summarised in table 1.

$$R^2 = 1 - \frac{\sum_i (y_i - {y'}_i)^2}{\sum_i (y_i - \frac{1}{n}\sum_{i=1}^{n} y_i)^2} \quad (14)$$

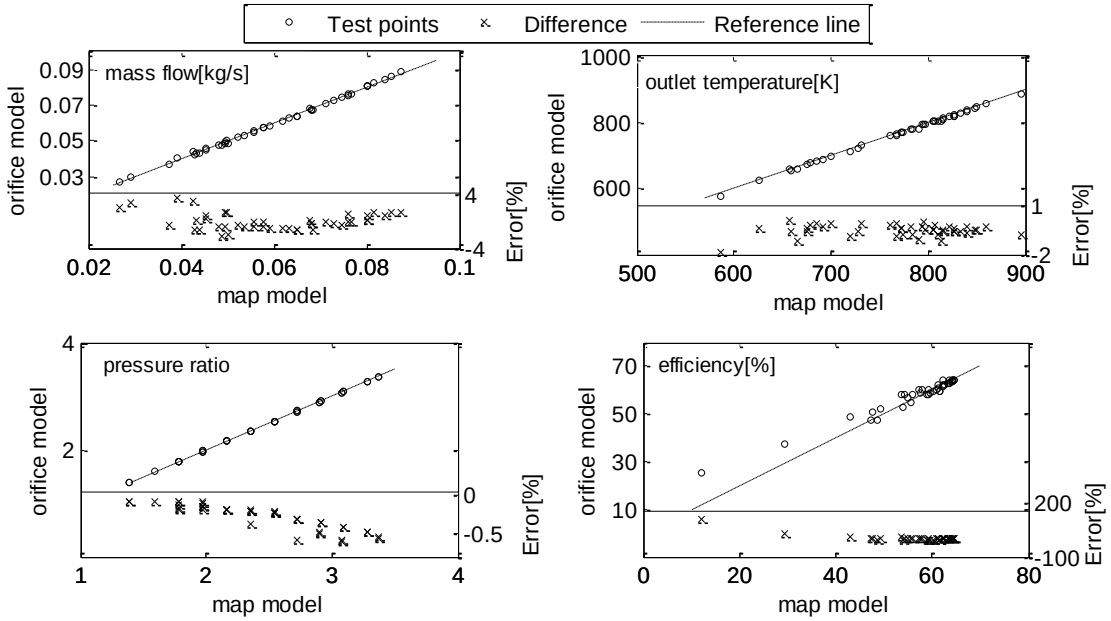

Figure 7: Dual-orifice model validation comparing dual orifice model with map based data

Table 1. Dual-orifice model evaluation

Parameter	Maximum Error (%)	R^2
Mass Flow	4	0.9937
Outlet Temperature	2	0.9894
Pressure Ratio	0.6	0.9997
*Efficiency	8	0.8995

* ignoring efficiency less than 40%

For efficiency, the best correlation was obtained closest to peak efficiency. Several points with large differences were found at low efficiency where the quality of the extrapolation is also poor. Overall, the dual-orifice model provides good correlation for steady operating points and will be carried forward for the transient simulations. A further dynamic validation would ideally be performed but is beyond the scope of this paper due to the experimental challenges of transient temperature and mass flow measurements.

3.2.2 Heat transfer model

The parameterisation and validation of the heat transfer model is inherited from a previous publication [39] for a different turbocharger. The heat transfer model has not been specifically validated experimentally for the turbocharger in this study, but rather the parameters have been translated through either the physical dimensions or through the use of model coefficients that have been shown to apply reasonably well to a range of turbocharger sizes and designs.

3.2.3 Waste-gate model

A dedicated test rig was constructed to parameterise the waste-gate actuator model as shown in figure 8. A pressure regulator was used to actuate the mechanical system whilst a laser position sensor was used to measure the opening of the waste-gate. It should be noted that these experiments were performed without aerodynamic loading of the waste-gate.

A series of steps in vacuum pressure were applied between maximum and minimum pressures causing step response of the actuator positions. The measured actuator position is shown in figure 9a along with the simulated results after fitting the damping ratio model parameter (b in equation 12). The root-mean-square error (RMSE) for the complete simulation was 0.16mm (calculated using equation 15) and R^2 was 0.99.

$$RMSE = \sqrt{\frac{\sum_{t=1}^{n}(y'_i - y_i)^2}{n}} \qquad (15)$$

Figure 9b shows details for two individual steps highlighting the transient response. Any errors here may be caused by simplification of the damping coefficient which was assumed to be constant.

The waste-gate area model was compared conceptually against data published in [46] and confirmed to provide a reasonable estimate of waste-gate area.

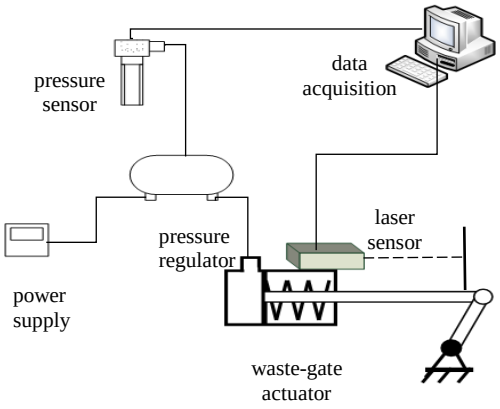

Figure 8: Schematic of the waste-gate actuator test rig

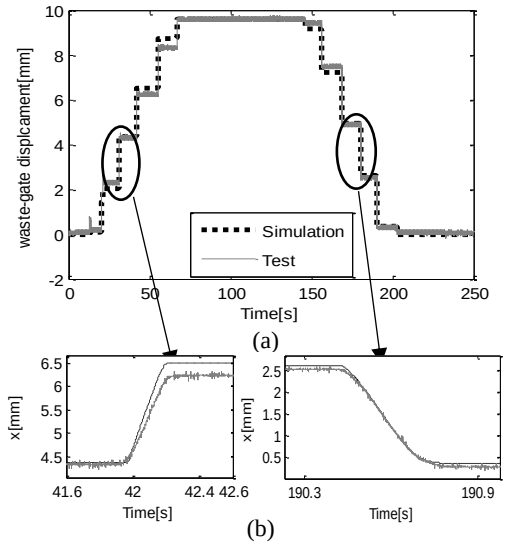

Figure 9: Measured and simulated waste gate actuator displacement (x)

3.3 Simulation conditions and Excitation signal design

The turbocharger turbine model was simulated under a range of transient boundary conditions covering a wide frequency range. Table 2 details the five simulation cases that were considered. Cases 1-3 were artificial excitations of individual variables: turbine inlet temperature (T_3), inlet stagnation pressure (P_3) and waste-gate actuator pressure (P_{vac}) whilst maintaining the other variables at constant. Cases 4 and 5 combined multiple excitations to provide conditions more representative of on-engine conditions.

Table 2. Simulation cases showing variable that were subjected to transient excitation and fixed magnitude of other variables

Case No.	1	2	3	4	5
T_3[K]	√	750	750	√	√
P_3[bar]	2.8	√	2.8	√	√
P_{vac}[bar]	0.1	0.1	√	0.1	√

The excitation signals for each variable were designed to be pure sine waves at ten distinct frequencies: 0.003Hz, 0.01Hz, 0.1Hz, 1Hz, 10Hz, 50Hz, 100Hz, 160Hz, 300Hz and 500Hz. This range has been chosen to cover the broad range of dynamics experienced by the turbocharger:

- At low frequencies the engine can require in the order of 10min to stabilise thermally (equivalent to a frequency of 0.001Hz)
- At the high frequencies, flow pulsations resulting from the opening and closing of the engine's exhaust depend on number of cylinders and engine speeds. For a four stroke, 4 cylinder engine operating at 6500rpm with two valve openings per revolution, the excitation frequency on the turbine would be 216Hz.

The amplitude of each signal was determined based on previous experimental tests from operating conditions on a typical gasoline engine: these are summarised in table 3.

Table 3. Amplitude ranges for transient signals for each input parameter

Signal Name	Signal Range
T_3[K]	500-1000
P_3[bar]	1.5-3.1
P_{vac}[bar]	0.3-1

Figure 10 shows the normalised excitation signals for selected frequencies (for clarity, not all frequency cases have been plotted). These have been plotted using a logarithmic time axis to highlight the range of frequencies that have been examined. In figure 10, the amplitude is normalised from 0 to 1 to illustrate the frequency ranges of the input signals, however in practice these are scaled according to the ranges detailed in table 3.

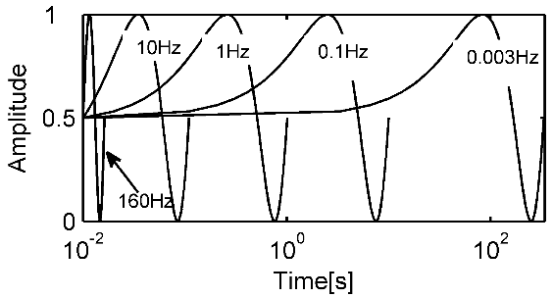

Figure 10: Normalised excitation signals for selected frequencies (note log scale on time axis)

4. RESULTS & DISCUSSION

The results in this sections are first organized according to the individual cases described in table 2. In a final section, a frequency based analysis is presented to link the findings to simulations tools and scenarios.

4.1 Inlet Temperature variations (Case 1)

The results presented in this section correspond to those with only turbine inlet temperature variation (case 1 in table 2). Figure 11 shows the time based turbine mass flow, turbocharger speed and wall temperature as a result of the excitation in inlet gas temperature.

For an ideal compressible gas, the mass flow rate could be calculated using equation 16. According to equation 16, the mass flow rate is expected to be inversely proportional to temperature. The results shown in figure 11b do follow this trend. As the input excitation frequency increases, the mass flow fluctuations have a greater higher amplitude which is consistent with previous studies on pulsating flows from literature. This might be caused by the wave interference. The superposition of incident wave and reflection wave form a resultant wave with amplitude greater or lower which is dependent on the phase difference between two waves.

$$\dot{m} = \frac{A_{pipe} P}{\sqrt{T}} f(R, \gamma, M) \qquad (16)$$

Figure 11c and 11d show the turbo shaft speed and turbine housing temperature. At low frequency, the shaft speed varies with an amplitude of around 18krpm as a result of variation in the enthalpy caused by changes in inlet temperature. As the frequency increases, the variation in shaft speed reduces because of the shaft inertia, until ultimately, with sufficiently high frequency, there is no fluctuation in shaft speed. A similar behaviour is observed for the turbine housing temperature but at lower frequencies due to the thermal inertia.

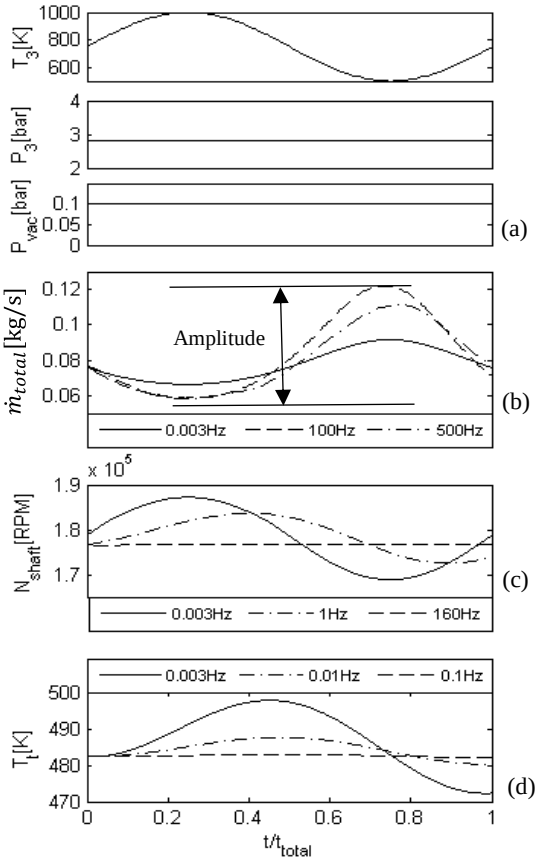

Figure 11. (a) Inlet parameters, (b) turbine mass flow, (c) turbo speed and (d) turbine housing temperature for Temperature only variation (case 1)

4.2 Inlet pressure variations (Case 2)

Figure 12a shows the boundary conditions used in this case: only inlet pressure was perturbed whilst inlet temperature and waste-gate position were held constant.

Figure 12b shows that the fluctuation of pressure at turbine inlet causes a fluctuation in mass flow rate, with higher pressures increasing the mass flow as a result of larger pressure ratio. As the frequency increases, higher amplitude of mass flow is observed.

The changes in turbocharger speed are plotted in figure 12c. At 0.003Hz, a maximum amplitude of approximately 40000rpm can be seen. As for the temperature variations, the mechanical inertia attenuates this variation as frequency is increased. At .160Hz, there is no change in turbocharger shaft speed as a result of the variation in inlet pressure.

The changes in mass flow affects the heat transfer to the turbine housing as shown in figure 12d. For the lowest frequencies, 10K variation is observed however at higher frequencies the thermal inertia again dominates, resulting in little variation in housing temperature.

4.3 Waste-gate pressure variation (Case 3)

In case 3, the inlet temperature and inlet pressure were both set to be constant at 750K and 2.8bar respectively whilst the vacuum pump pressure supplied to the actuator was varied between 0.3bar to 1bar. These boundary conditions are plotted in figure 13a.

The change in vacuum pressure causes the waste-gate to open and close (evidenced by the change in waste-gate diameter, figure 13b). At a frequency of 0.003Hz, the waste-gate actuator has time to respond to the changes in vacuum pressure and fully opens and closes during the first half of the sine period. The waste-gate is fully closed during the second half as the vacuum pressure is too high to allow opening.

As frequency increases, the waste-gate can no longer fully open: a reduction in amplitude and significant phase lag are obvious at 50Hz. For a frequency of 500Hz, the waste-gate stays closed throughout.

As figure 13c shows, the mass flow through the turbine wheel reduces when the waste-gate opens. However, with constant inlet pressure and temperature, the total mass flow entering the turbine that flows through both the waste-gate and rotor wheel increases (figure 13d).

It should be noted that as the inlet pressure and temperature are imposed in this simulation, a different behaviour than would be expected on-engine is observed. For engine applications, the opening of waste-gate would reduce the turbine inlet pressure.

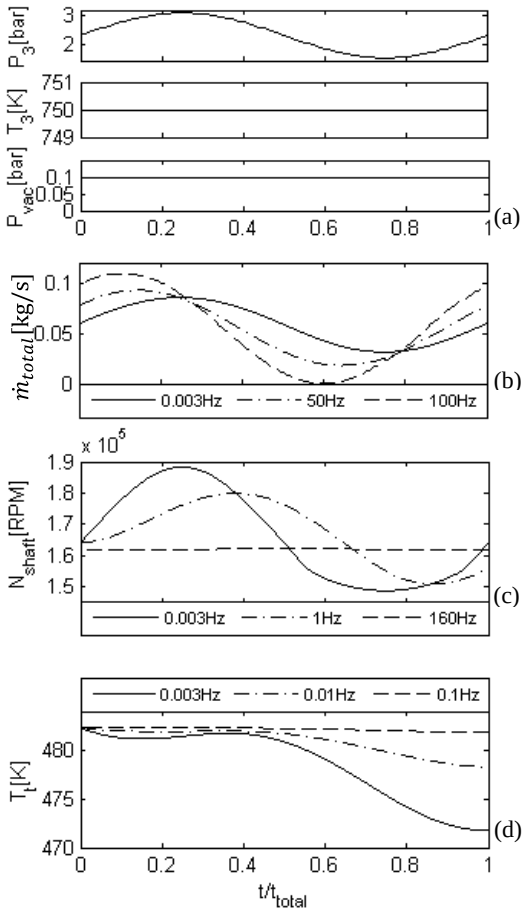

Figure 12. (a) Inlet parameters, (b) turbine mass flow, (c) turbo speed and (d) turbine housing temperature for pressure only variation (case 2)

The changes in turbine housing temperature are explained by changes to the convective heat transfer coefficient as a result of the fluctuations in mass flow. The increase in total mass flow results in an increase in convection between the turbine wall and fluids.

Greater heat transfer tends to increase the turbine housing temperature (figure 13e). In figure 13f, the decrease of turbo speed is caused by the reduction of mass flow through the rotor.

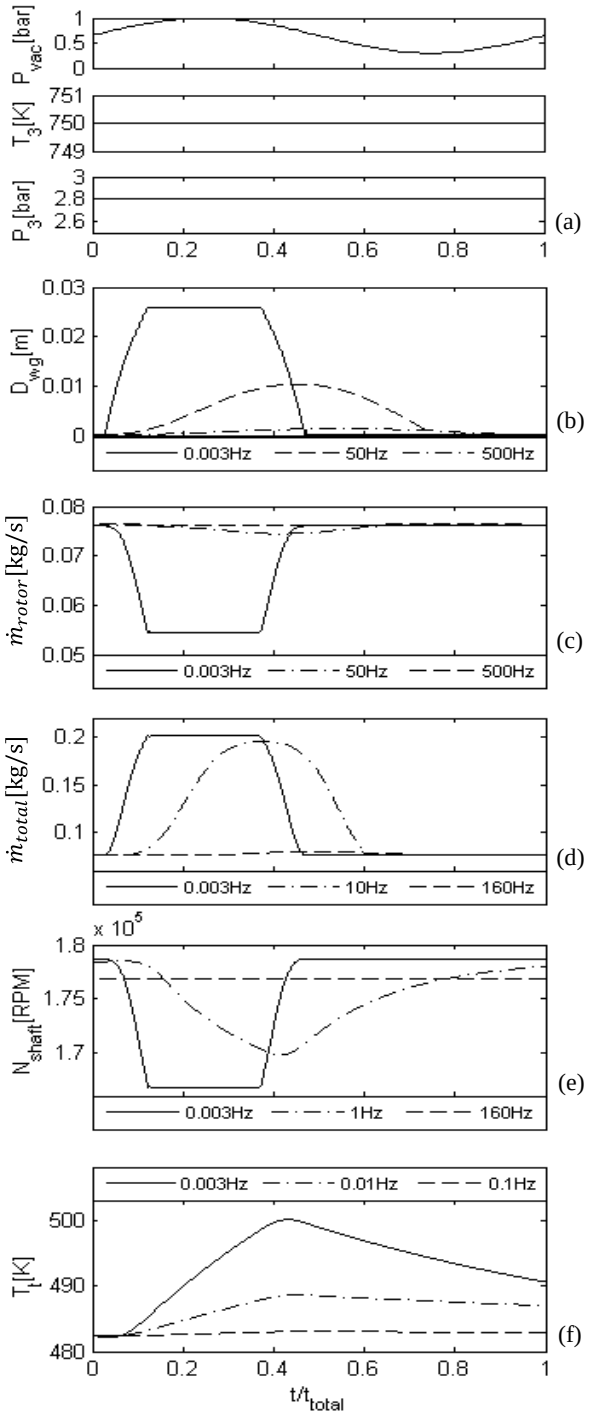

Figure 13: (a) Inlet parameters, (b) waste-gate effective diameter, (c) mass flow through rotor, (d) mass flow through volute, (e) turbo speed and (f) turbine wall temperature for actuator pressure only variation (case 3)

4.4 Combined variations (case 4& 5)

In case 4, both temperature and pressure were varied while the waste-gate remained closed. The main effects of the turbine elements had similar trends to the variations of individual parameters presented in the previous sections (cases 1 to 3). In case 5, all three parameters were varied simultaneously.

Figures 14a and 15a illustrate the boundary conditions set in case 4 and 5 respectively. With more than one boundary varied at the same time, the effects on the system become more complex and depend on the relative frequencies and phases between inputs. These simulation cases do not therefore pretend to cover the full range of possible conditions, but rather to exemplify the behaviour in the presence of simultaneous changes in boundary conditions.

As shown in figures 14b and 14c, the mass flow and turbocharger speed no longer vary as pure sine waves for all frequencies as was the case for individual variations of inlet temperature or pressure.

For mass flow, the shape of the curves in figure 14c can be explained by considering the results from figures 11b and 12b. At low frequency, the variations in mass flow are predominantly due to fluctuations in pressure. However, as the frequency of the fluctuations increases, there is an increasing effect from temperature.

Within the frequency range not affected by shaft inertia, the amplitude of turbocharger speed (figure 14b) is greater than the amplitude of individual fluctuations of temperature (figure 11c) and pressure (figure 12c). There is a combined effect of pressure and temperature changes that are in phase with each other.

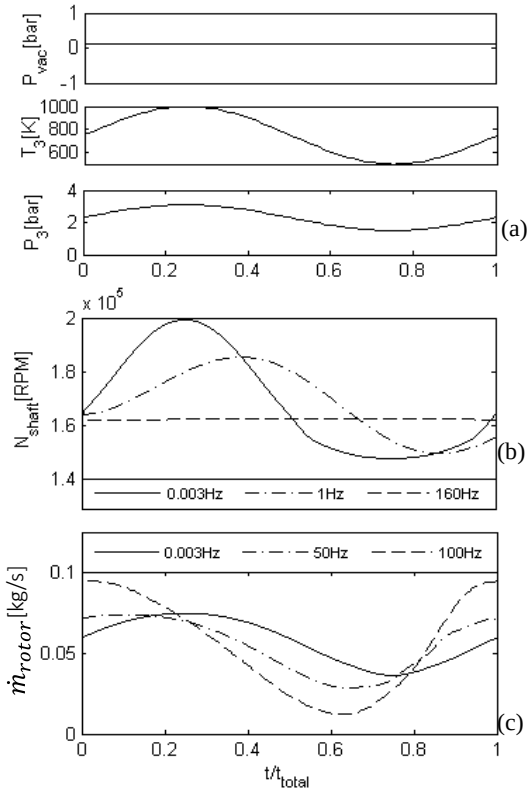

Figure 14: (a) Inlet parameters, (b) turbo speed and (c) mass flow through rotor for temperature and pressure variations (case 4)

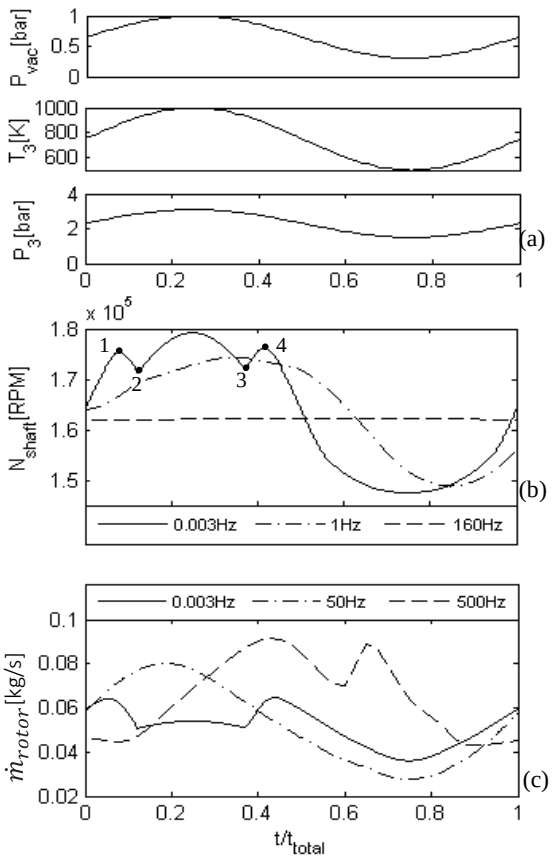

Figure 15: (a) Inlet parameters, (b) turbo speed and (c) mass flow through rotor for all parameters variation (Case 5)

When the waste gate is also actuated as shown in figure 15, the effect of the waste-gate actuator is in effect superimposed onto the inlet temperature and pressure effects. As the frequency increases, the response to the waste-gate exhibits a larger phase shift and is attenuated until ultimately there is no effect from the waste-gate actuator vacuum pressure.

Considering the calculated turbo shaft speed at low frequency (figure 15b), at point 1, waste-gate started to open and the mass flow through the turbine dropped, resulting in a decrease in turbo speed. The waste-gate is fully open between points 2 and 3: during this time, turbo shaft speed increases following the increase of temperature and pressure. Between point 3 and 4, waste-gate closes, thus increasing the mass flow through the rotor and also the turbo shaft speed. Before point 1 and after point 4, the waste-gate is fully closed, and the results are similar to those in figure 14b.

4.5 Frequency domain analysis

In order to compare turbine behaviour across the frequency spectrum, for each simulation case the amplitude was calculated according to equation 17. Amplitude is defined as the difference between the maximum and minimum value of the signal over a single period as illustrated in figure 11b.

$$\text{Amplitude} = \max(\text{signal}) - \min(\text{signal}) \qquad (17)$$

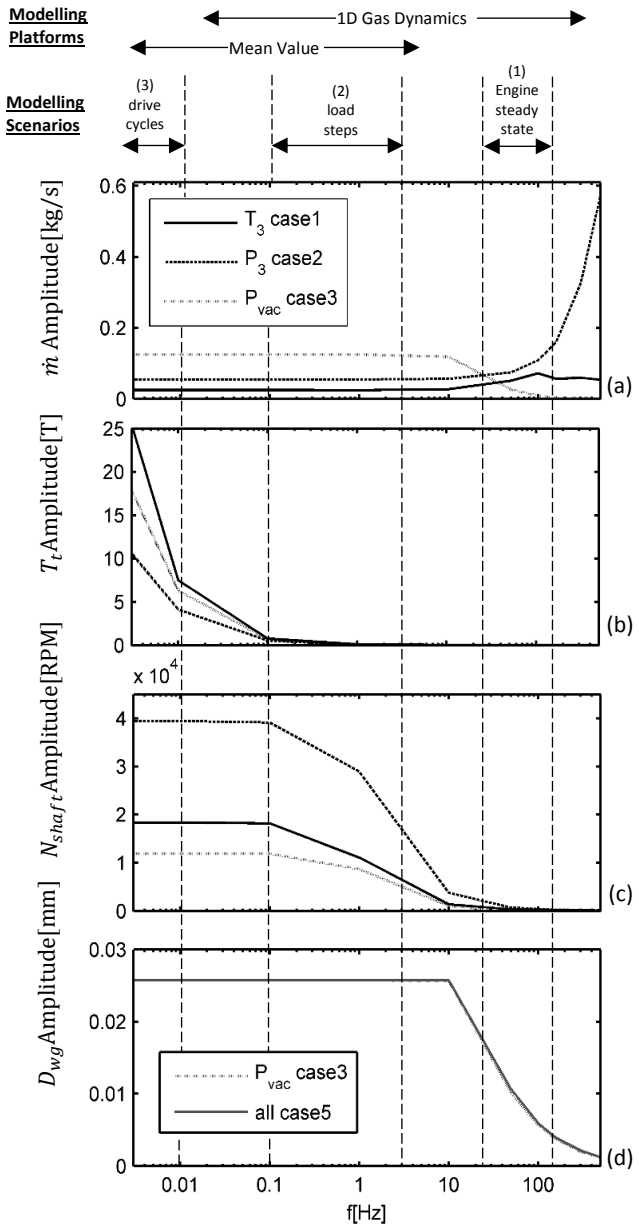

Figure 16: (a) Mass flow (b) Turbine wall temperature (c) Turbo speed (d) Waste-gate effective diameter amplitude across the frequency spectrum for all cases

Figure 16a shows the amplitude of mass flow fluctuations across the frequency range for cases 1-3. At lower frequencies, the waste-gate actuator pressure causes a higher amplitude than the inlet pressure or inlet temperature. For frequencies above 80Hz, the response due to waste-gate actuator pressure reduces, caused by the mechanical inertia of the system whilst the response to temperature and pressure increase caused by interactions between forward and reflected waves at high frequency. This indicates that at these higher frequencies, it is inappropriate to treat turbine model as a quasi-steady manner.

The same response for turbine housing temperature is shown in figure 16b for cases 1-3. The largest effect comes from temperature fluctuations but the amplitude will depend on mass flow and pressure too. For frequencies above 0.1Hz, there is almost no change in housing temperature.

Figure 16c shows the turbo speed amplitude. Similar to the thermal inertia for housing temperature, the mechanical inertia causes a reduction in amplitude above 0.1Hz and full attenuation is reached by 10Hz.

In figure 16d, the waste-gate actuator response is shown by plotting the amplitude of waste-gate effective area: these results illustrate the performance of the pneumatic actuator and mechanical linkage mechanism. Only cases 3 and 5 are illustrated as the other simulation cases were performed with waste-gate closed. The mass of the actuator system limits the waste-gate area control for frequencies above 50Hz.

These frequency based results can be used to determine the importance of certain model parameters that influence the dynamic response for particular simulation problems. These parameters include mechanical inertias, internal volumes and thermal capacities. Three different simulation scenarios can be considered below. The frequency range of these scenarios is indicated in figure 16. Also indicated are the typical frequency ranges of interest for two key modelling approaches: 1D Gas dynamics and Mean value (1 value per cycle) engine models.

SCENARIO 1: *Steady state engine condition simulations: the excitation frequency as a result of valve events is in the range of 25 to 150Hz*

At these frequencies, the turbine casing temperature and turbo speed do not react to the rapid changes of the boundary conditions as shown in figure 16b and 16c. This means that poor estimates in mechanical and thermal inertia will have little effect on the modelling accuracy and a constant estimation of housing temperature or shaft speed will remain accurate. In contrast, significant mass flow fluctuations were obtained as shown in figure 16a, which will highly influence the turbine instantaneous mass flow and have knock-on effects for efficiency and power estimation.

SCENARIO 2: *An engine load transient or individual vehicle manoeuver will excite the turbocharger system in the frequency range of 0.1Hz and 3Hz.*

Before discussing this scenario, it should be noted that this situation is commonly simulated in 1D gas dynamic codes that solve equations describing engine operation on a crank angle basis. Therefore such a simulation inherits the requirements of the frequency range described in scenario 1, but in addition must consider the additional parameters discussed below. In this frequency range, the mass flow behaviour shown in figure 16a indicates that the mass flow will respond in much a quasi-steady way. The wall temperature response (figure 16b) remains low in this frequency range, meaning the precise determination of thermal masses is of lower importance. In contrast, the turbocharger speed (figure 16c) exhibits a wide variation across this frequency range, highlighting the importance of shaft inertia for the simulation of these events. The waste gate actuator (figure 16d) does not have a significant dynamic effect either in this range, meaning the transient parameters such as actuator and linkage masses are less crucial.

It is important to note the significance but also limitation of these results:

- The results are showing that the change in turbine housing temperature during this type of load step is not important for simulation accuracy. Therefore the estimate of housing thermal inertia is not a crucial model parameter.
- The results are not suggesting that heat transfer is not important during the transient event, and this would be reflected through an imposed turbine wall temperature at the start of the simulation.

SCENARIO 3: *Cold start drive cycles are important for vehicle pollutant emissions prediction. The warm-up period is usually 1-10min (depending on the fluid in question and the start temperature), making the excitation frequency range from 0.01Hz to 0.003Hz.*

The timescales are much larger than the dynamics of the mass flow waste-gate actuator and turbo shaft speed meaning that parameters for these are less critical. The wall temperature does have an important effect on transient response as shown in figure 16b. For this transient condition, the thermal inertia will be a critical model parameter.

5. CONCLUSION

By using a combination of advanced dynamic models of three key elements of the turbocharger turbine, the dynamic response of the system has been evaluated across a broad frequency range. By imposing artificial input signals at the boundaries of turbine inlet pressure, temperature and waste-gate actuator vacuum, the dynamic response of the mechanical, thermal and fluid mechanical elements were estimated. The turbine mass flow response was mostly affected by variations in turbine inlet pressure and temperature above a frequency of 10Hz and more significantly above 100Hz. The waste-gate actuator exhibited significant dynamic effects, primarily due to its mechanical inertia, also for frequencies above 10Hz. The mechanical inertia of the turbine shaft was most significant for frequencies ranging 0.1-10Hz, with no fluctuations in shaft speed observed above 10Hz. Finally, the thermal inertia of the turbocharger housing meant that housing temperature fluctuations were supressed for excitation frequencies above 0.01Hz.

Further work should apply the methods developed here to a broader range of operating conditions and varying sized turbochargers. Whilst this would allow wider applicability, the results presented here do give an appreciation of the system behaviour for small automotive sized turbochargers. The results have been used to determine the importance of model parameters controlling the system dynamics for three different simulation scenarios.

6. NOMENCLATURE

Acronyms

PR	Pressure ratio
$RMSE$	root mean square deviation

Symbols

A	Area (m^2)
c_p	specific heat at constant pressure $(J/kg \cdot K)$
D	diameter (m)
F	Force (N)
f	Frequency (Hz)

h	Convective heat transfer coefficient (W/m^2K)
I	Moment of inertia (kgm^2)
k	Thermal Conductivity (W/mK) Spring stiffness (N/m)
l	Length (m)
$\dot{m}$	mass flow rate(kg/s)
N	Speed (RPM)
Nu	Nusselt number
n	number of data points
P	stagnation pressure(bar)
Pr	Prandtl number
Q	Heat transfer rate (W)
R	Radius (m)
R^2	determination of coefficient
Re	Reynolds number
T	temperature(K)
t	Time (s)
t_{total}	total time of simulation (s)
W	power (w)
x	Displacement of waste gate actuator from position of Pvac=Pamb
y	experimental test data
y'	simulated data

Greek symbol

β	angle of waste-gate poppet (rad)
γ	Ratio of specific heats
ε	emissivity
σ	Stefan-Boltzmann constant($W/m^2 \cdot K^4$)
μ	Dynamic Viscosity (Ns/m^2)

Subscripts

amb	ambient
BH	Bearing housing
C	Compressor Housing
c	compressor
gas	Working fluid
HP	High pressure side
LP	Low pressure side
oil	turbocharger lubricant oil
$piston$	piston of waste-gate actuator
pre	waste-gate preload
rad	Radiation
$shaft$	turbocharger shaft
T	Turbine housing
t	turbine
$turbo$	turbocharger
vac	vacuum of waste-gate actuator
$valve$	Waste-gate valve
wg	waste-gate
1	Pre compressor
2	Post compressor
3	Turbine stage inlet
$3'$	Pre turbine expansion, post turbine heat transfer,
4	Rotor inlet

5	Rotor Outlet
5′	Post turbine expansion, post turbine heat transfer
6	Turbine stage outlet

7. ACKNOWLEDGEMENT

The authors would like to thank China Scholarship Council and Honeywell for supporting this project and Calo Avola for his assistance with the waste-gate test rig.

8. REFERENCES

[1] Copeland, C., Newton, P., Martinez-Botas, R., and Seiler, M., 2012, "A comparison of timescales within a pulsed flow turbocharger turbine," Proceedings of IMechE, Paper(C1340/086), pp. 389-404.
[2] Martin, G., Talon, V., Higelin, P., Charlet, A., and Caillol, C., 2009, "Implementing turbomachinery physics into data map-based turbocharger models," SAE International Journal of Engines, 2(1), pp. 211-229.
[3] Payri, F., Benajes, J., and Reyes, M., 1996, "Modelling of supercharger turbines in internal-combustion engines," International Journal of Mechanical Sciences, 38(8-9), pp. 853-869.
[4] De Bellis, V., Marelli, S., Bozza, F., and Capobianco, M., 2014, "Advanced Numerical/Experimental Methods for the Analysis of a Waste-Gated Turbocharger Turbine," SAE International Journal of Engines, 7(1), pp. 145-155.
[5] MacEk, J., and Vitek, O., 2008, "Simulation of pulsating flow unsteady operation of a turbocharger radial turbine," Proc. 2008 World Congress, April 14, 2008 - April 17, 2008, SAE International.
[6] Aymanns, I. R., Scharf, I. J., Uhlmann, D.-I. T., and Pischinger, I. S., 2012, "Turbocharger Efficiencies in Pulsating Exhaust Gas Flow," MTZ worldwide, 73(7-8), pp. 34-39.
[7] Costall, A., Szymko, S., Martinez-Botas, R. F., Filsinger, D., and Ninkovic, D., 2006, "Assessment of Unsteady Behavior in Turbocharger Turbines," Proc. ASME Turbo Expo 2006: Power for Land, Sea, and Air, American Society of Mechanical Engineers, pp. 1023-1038.
[8] Costall, A., Rajoo, S. and Martinez-Botas, R. F., 2006, "Modelling and Experimental Study of the Unsteady Effects and their Significance for nozzleless and nozzled Turbine Performance," THIESEL Conference on Thermo and Fluid Dynamic Processes in Diesel Engines.
[9] Benson, R. S., 1974, "Nonsteady flow in a turbocharger nozzleless radial gas turbine," Proc. National Combined Farm, Construction and Industrial Machinery and Powerplant Meetings, September 9, 1974 - September 12, 1974, SAE International.
[10] Wallace, F., and Blair, G., 1965, "The pulsating-flow performance of inward radial-flow turbines," Proc. ASME 1965 Gas Turbine Conference and Products Show, American Society of Mechanical Engineers, pp. V001T001A021-V001T001A021.
[11] Wallace, F., and Miles, J., 1970, "Performance of inward radial flow turbines under unsteady flow conditions with full and partial admission," Proceedings of the Institution of Mechanical Engineers, 185(1), pp. 1091-1105.
[12] Kosuge, H., Yamanaka, N., Ariga, I., and Watanabe, I., 1976, "Performance of radial flow turbines under pulsating flow conditions," Journal of Engineering for Gas Turbines and Power, 98(1), pp. 53-59.
[13] Capobianco, M., and Marelli, S., 2007, "Waste-Gate Turbocharging Control in Automotive SI Engines: Effect on Steady and Unsteady Turbine Performance," SAE International.
[14] Capobianco, M., and Marelli, S., 2010, "Experimental investigation into the pulsating flow performance of a turbocharger turbine in the closed and open waste-gate region," Proc. 9th International Conference on Turbochargers and Turbocharging, May 19, 2010 - May 20, 2010, Woodhead Publishing Ltd., pp. 373-385.
[15] Capobianco, M., and Polidori, F., 2008, "Experimental Investigation on Open Waste-Gate Behaviour of Automotive Turbochargers," SAE International.
[16] Capobianco, M., and Marelli, S., 2011, "Experimental analysis of unsteady flow performance in an automotive turbocharger turbine fitted with a waste-gate valve," Proceedings of the Institution of Mechanical Engineers, Part D: Journal of Automobile Engineering, 225(8), pp. 1087-1097.
[17] Szymko, S., Martinez-Botas, R., and Pullen, K., 2005, "Experimental evaluation of turbocharger turbine performance under pulsating flow conditions," Proc. ASME Turbo Expo 2005: Power for Land, Sea, and Air, American Society of Mechanical Engineers, pp. 1447-1457.
[18] Watson, N., 1982, Turbocharging the internal combustion engine, London : Macmillan, London.
[19] Payri, F., Desantes, J.M. and Boada, J., 1986, "Prediction method for the operating conditions of a turbocharged Diesel engine," Proc. Proceedings of the motor symposium, Prague, vol. 2, 1986, pp. 8-16.
[20] Winterbone, D., 1990, "The theory of wave action approaches applied to reciprocating engines," Internal Combustion Engineering: Science & Technology, Springer, pp. 445-500.

[21] Baines, N. C., Hajilouybenisi, A. and Yeo, J. H., 1994, "THE PULSE FLOW PERFORMANCE AND MODELING OF RADIAL INFLOW TURBINES," Proc. Turbocharging and Turbochargers: International Conference, Mechanical Engineering Publication, pp. 209-219.
[22] Kessel, J. A., Schaffnit, J., and Schmidt, M., 1998, "Modelling and real-time simulation of a turbocharger with variable turbine geometry (VTG)," Proc. 1998 SAE International Congress and Exposition, February 23, 1998 - February 26, 1998, SAE International.
[23] Nasser, S. H., and Playfoot, B. B., 1999, "A Turbocharger Selection Computer Model," SAE International.
[24] Serrano, J., Arnau, F., Dolz, V., Tiseira, A., and Cervelló, C., 2008, "A model of turbocharger radial turbines appropriate to be used in zero-and one-dimensional gas dynamics codes for internal combustion engines modelling," Energy Conversion and Management, 49(12), pp. 3729-3745.
[25] Marelli, S., and Capobianco, M., 2009, "Measurement of Instantaneous Fluid Dynamic Parameters in Automotive Turbocharging Circuit," 9th International Conference on Engines and Vehicles, Consiglio Nazionale delle Ricerche, Capri, Naples, Italy.
[26] Galindo, J., Climent, H., Guardiola, C., and Doménech, J., 2009, "Modeling the Vacuum Circuit of a Pneumatic Valve System," Journal of Dynamic Systems, Measurement, and Control, 131(3), pp. 031011-031011.
[27] Messina, A., Giannoccaro, N. I., and Gentile, A., 2005, "Experimenting and modelling the dynamics of pneumatic actuators controlled by the pulse width modulation (PWM) technique," Mechatronics, 15(7), pp. 859-881.
[28] Sorli, M., Gastaldi, L., Codina, E., and de las Heras, S., 1999, "Dynamic analysis of pneumatic actuators," Simulation Practice and Theory, 7(5–6), pp. 589-602.
[29] Thomasson, A., Eriksson, L., Leufven, O., and Andersson, P., 2009, "Wastegate actuator modeling and model-based boost pressure control," Proc. IFAC Workshop on Engine and Powertrain Control, Simulation and Modeling, Paris, November, pp. 87-94.
[30] Serrano, J., Olmeda, P., Arnau, F., Reyes-Belmonte, M., and Lefebvre, A., 2013, "Importance of heat transfer phenomena in small turbochargers for passenger car applications," SAE Technical Paper.
[31] Mrosek, M. a. I., R., 2010, "On the Parametrisation of the Turbocharger Power and Heat Transfer Models," IFAC AAC 2010Munich, Germany.
[32] Shaaban, S., 2004, "Experimental Investigation and Extended Simulation of the Turbocharger Power and Heat Transfer Models," Ph.D., University of Hannover, Germany.
[33] Casey, M. V., and Fesich, T. M., 2010, "The efficiency of turbocharger compressors with diabatic flows," Journal of Engineering for Gas Turbines and Power, 132(7).
[34] Sirakov, B., and Casey, M., 2012, "Evaluation of Heat Transfer Effects on Turbocharger Performance," Journal of Turbomachinery, 135(2), pp. 021011-021011.
[35] Romagnoli, A., and Martinez-Botas, R., 2012, "Heat transfer analysis in a turbocharger turbine: An experimental and computational evaluation," Applied Thermal Engineering, 38(0), pp. 58-77.
[36] Romagnoli, A., and Martinez-Botas, R., 2009, "Heat transfer on a turbocharger under constant load points," Proc. 2009 ASME Turbo Expo, June 8, 2009 - June 12, 2009, American Society of Mechanical Engineers, pp. 163-174.
[37] Chesse, P., Chalet, D., and Tauzia, X., 2011, "Impact of the Heat Transfer on the Performance Calculations of Automotive Turbocharger Compressor," Oil & Gas Science and Technology–Revue d'IFP Energies nouvelles, 66(5), pp. 791-800.
[38] Nakhjiri, M., Pelz, P. F., Matyschok, B., Däubler, L., and Horn, A., 2012, "Apparent and Real Efficiency of Turbochargers under Influence of Heat Flow," 14th International Symposium on Transport Phenomena and Dynamics of Rotating Machinery, February 27, 2012 – March 2, 2012, Honolulu,USA.
[39] Burke, R. D., 2013, "Analysis and modelling of the transient thermal behaviour of automotive turbochargers," Proc. ASME 2013 Internal Combustion Engine Division Fall Technical Conference, ICEF 2013, October 13, 2013 - October 16, 2013, American Society of Mechanical Engineers (ASME), p. Internal Combustion Engine Division.
[40] Serrano, J. R., Olmeda, P., Arnau, F. J., Dombrovsky, A., and Smith, L., 2015, "Turbocharger heat transfer and mechanical losses influence in predicting engines performance by using one-dimensional simulation codes," Energy, 86, pp. 204-218.
[41] Payri, F., Serrano, J., Fajardo, P., Reyes-Belmonte, M., and Gozalbo-Belles, R., 2012, "A physically based methodology to extrapolate performance maps of radial turbines," Energy Conversion and Management, 55, pp. 149-163.
[42] Olmeda, P., Dolz, V., Arnau, F. J., and Reyes-Belmonte, M. A., 2013, "Determination of heat flows inside turbochargers by means of a one dimensional lumped model," Math. Comput. Model., 57(7-8), pp. 1847-1852.
[43] Burke, R., Copeland, C., Duda, T., and Reyes Belmonte, M., 2015, "Lumped capacitance and 3D CFD conjugate heat transfer modelling of an automotive turbocharger.". Proc. ASME Turbo Expo 2015: Turbine Technial Conference and Exposition, June 15, 2015 – June 19, 2015, American Society of Mechanical Engineers(ASME), pp. V008T23A004.
[44] Burke, R., Vagg, C., Chalet, D., and Chesse, P., 2015, "Heat transfer in turbocharger turbines under steady, pulsating and transient conditions," International Journal of Heat and Fluid Flow, 52, pp. 185-197.
[45] Eriksson, L., 2002, "Mean Value Models for Exhaust System Temperatures," SAE International.
[46] Toussaint, L., Marques, M., Morand, N., Davies, P., Groves, C., Tomanec, F., Zatko, M., Vlachy, D., Mrazek, R., and Inst Mech, E., 2014, Improvement of a turbocharger by-pass valve and impact on performance, controllability, noise and durability, Woodhead Publ Ltd, Cambridge.

[47] Jensen, J. P., Kristensen, A. F., Sorenson, S. C., Houbak, N., and Hendricks, E., 1991, "Mean Value Modeling of a Small Turbocharged Diesel Engine," SAE International.